Kabiri, Ali, Liaghat, Gholamhossein, Alavi, Fatemeh, Saidpour, Hossein, Hedayati, Seyyed Kaveh, Ansari, Mehdi and Chizari, Mahmoud (2020) Glass fiber/ polypropylene composites with potential of bone fracture fixation plates : manufacturing process and mechanical characterization. Journal of Composite Materials, 54(30), pp. 4903-4919.
DOI: https://doi.org/10.1177%2F0021998320940367

Glass Fiber/Polypropylene composites with Potential of Bone Fracture Fixation Plates: Manufacturing Process and Mechanical Characterization

Ali Kabiri[a], Gholamhossein Liaghat[a, b, *], FatemehAlavi[a], Hossein Saidpour[c],SeyyedKavehHedayati[a], Mehdi Ansari[d], Mahmoud Chizari[c]

[a] *Faculty of Mechanical Engineering, Tarbiat Modares University, Tehran, Iran*

[b] *School of Mechanical & Aerospace Engineering, Kingston University, London, UK*

[c] *Engineering Department, University of Hertfordshire, London, UK*

[d] *Department of Mechanical Engineering, Arak University of Technology, Arak, Iran*

Abstract

Mechanical properties and manufacturing processes of Glass Fiber/Polypropylene (GF/PP) composites for application of flexible internal long bone fracture fixation plates have been investigated. PP/Short Chopped Glass Fiber (PPSCGF), PP/Long Glass Fiber (PPLGF) and PP/Long Glass Fiber Yarn (PPLGFY) were used in fabrication of the fixation plates. The PPSCGF and PPLGF plates were made by the heat-compressing process and Three-dimensional (3D) printing method was used to make the PPLGFY ones. The values of Young's modulus, tensile strength, flexural modulus and strength, and impact strength of the PPSCGF in the fiber longitudinal direction were found to be 2.35 ± 0.15 GPa, 30 ± 5 MPa, 2.1 ± 0.2 GPa, 27 ± 5 MPa and 22 ± 5 kJ/m^2, respectively. Where, these values for the PPLGF were to 20.10 ± 2GPa, 400 ± 30MPa, 16.2 ± 0.2GPa, 185 ± 5MPa, and 162 ± 5kJ/m^2 and for the PPLGFY were to 7.87 ± 0.5GPa, 150 ± 20MPa, 2.3 ± 0.2GPa, 44 ± 5MPa and $68 \pm$

*Corresponding author.

Gholamhossein Liaghat, TarbiatModares University, Jalal-e-Al-Ahmad,Tehran 14115111, Iran.

Email: ghlia530@modares.ac.ir, g.liaghat@kingston.ac.uk

5kJ/m^2. These have been found to be in close agreement with the human bone properties. Furthermore, the strength and modulus values of the plates were reasonable to be used as a bone implant applicable for bone fracture reconstructions. Hence, the study concluded that the GF/PP composites are useful for load-bearing during daily activities and would be recommended as a choice in orthopedic fixation plate applications. It will help the researchers for development of new fixation designs and the clinicians for better patient's therapy in future.
Keywords: Mechanical properties, Manufacturing process, Microscopic investigations, Fixation plate, GF/PP composite.

1. Introduction

Fracture fixation plate is the most popular device for healing bone fractures, in spite of the existence of other surgical devices such as pins, wires, screws, nails and rods. Conventional fixation plates are made of metals such as stainless steel, Co–Cr and titanium alloys [1]. The elastic modulus of the human cortical bone is about 20 GPa [2], while, the elastic modulus of the conventional metallic fixation plates is much higher than the cortical bone. Since the high modulus of metallic fixation plates overprotects the bone, it may apply a large amount of stress to the bone during daily activities. This phenomenon called "Stress shielding" and may cause bone osteoporosis and in later stage remodel the bone. However, the plate with closer elastic modulus to the bone elastic modulus would allow the bone to take more stress and would overcome the stress shielding effect [3]. Also, any corrosion in the metallic plate would increase the accumulation of metallic particles in the vicinity of the implant, which may change osteoblast behavior even at sub-toxic levels, or at distant body parts including draining lymph nodes with likely allergic reactions in the spleen and liver [4]. In addition, metallic materials are particularly incompatible with medical imaging technologies such as computed

tomography (CT) scan and magnetic resonance imaging (MRI), because they appear white on the exposed film due to its radiopaque behavior [5].

To compensate for these negative effects, polymer-based composites have been introduced to be replaced with metallic plates due to their high strength-to-weight ratio, non-corrosiveness and radiolucency [5]. Moreover, it is possible to achieve optimum mechanical properties of the composite plates by controlling the fiber volume fraction, local and global arrangement of the fibers. Furthermore, bio-compatibility of the composite samples can be controlled, so the sample can be used for fixing a fractured bone with more advantages than metallic plates.

Although, early efforts on using thermoset polymers were unsuccessful due to toxic reactions, permanent physical irritation and chronic inflammatory local reactions in animals [5]. However, Ali et al. compared the mechanical properties of carbon fiber-reinforced epoxy with stainless steel and titanium composite fixation plates [6]. Their results showed less stiff composite plates have more favorable fatigue property than metallic plates. By investigating the animal samples, they found that using a composite plate reduced 67% of structural stiffness. In a recent investigation, researchers have used thermoplastic composites polymer to produce new fixation plate fixation. The thermoplastic polymers are more beneficial due to their bio-compatibility and degradation rates, which can be easily controlled by changing the composition and fabrication techniques. Fujihara et al. reported that the stiffness of Carbon Fiber/polyether ether ketone (CF/PEEK) is half of the steel stiffness but the static strength is the same [7 and 8]. Therefore, they proposed it as a replacement for metallic fixation plates which can reduce stress shielding. Thus, Huang and Fujihara investigated the influence of various aspects, such as fabrication conditions, braiding angle and plate thickness to improve the flexural performance of braided CF/PEEK composite fixation plates [9]. Also, Schambron et al. conducted static and cyclic bending tests on braided CF/PEEK fixation plates were in a simulated body environment and indicated that bending stiffness, strength failure modes

remained unchanged due to the body fluid effects [10]. In addition, Steinberg et al. studied the static and fatigue modes of the samples using a four-point bending method [11]. They also investigated the wear/debris characteristics of dynamic compression, proximal humeral, distal volar radial fixation plates and tibia nail made of CF/PEEK composite. Their results showed CF/PEEK devices could withstand one million fatigue cycles without failure. They also discovered that the generated particles in the composites plate during wear tests were found to be lower than those in metallic implants.

Along with the investigations performed on non-biodegradable composites, research on biodegradable reinforced polymer composites for internal fracture fixation is of interest to many researchers. Huda et al. investigated the mechanical and thermo-mechanical properties of developed Kenaf/polylactic acid (Kenaf/PLA) bio-composite [12]. They have studied the optimal manufacturing process between “alkalization” and “silane-treatments” by comparing impact strength, flexural properties and temperature curves of storage modulus, loss modulus, and loss factor in different samples. Also, Aydin et al. produced novel biodegradable hydroxyapatite nanorod-reinforcedpoly-L-lactic acid(PLLA) composites for fixation plates [13]. They investigated the samples in both in-vitro and in-vivo conditions and found the tensile and compressive properties of these composite plates. From their finding, they have indicated that compressive mechanical properties of these materials could be suitable for fixation plates. Li et al. studied the flexural strength, impact strength and in-vitro degradation behavior of unidirectional magnesium alloy wires/PLA composite using experimental and theoretical methods [14]. They found the degradation rate of PLA decreased by adding treated magnesium alloy wires using the micro-arc oxidation technique. In other research, Santos et al. evaluated thermal stability, crystallinity, transition temperatures, maximum flexural load and storage modulus of the fixation plates composed of polylactic-co-glycolic acid (PLGA) polymer matrix and combinations of calcium phosphates bio-ceramics [15]. The proposed optimum ceramic's

mass values for improving the thermal and mechanical properties of bio-ceramics/PLGA composite fixation plates.

Several researchers reported about reinforcement using glass fibers. They concluded that the glass fibers maintain stability in polymers and improve their mechanical properties such as damage tolerance, fracture toughness and fatigue performance [16 and 17]. For bone fracture fixation devices, Jiang et al. have studied the effects of polymerization on Young's modulus and flexural strength ofBioGlass/polycapro-lactone(BioGlass/PCL) fiber composite for bone implant applications [18]. Kobayashi et al. investigated mechanical properties and pH changing in physiological solutions of degradable organic polymer networks based on methacrylate-modified oligolactide and calcium carbonate when reinforced by phosphate glass fibers [19]. Also, Ahmed et al. investigated mechanical properties, scanning electron microscope (SEM) analyses, degradation and pH changing studies of PLA/phosphate glass fiber reinforced composites [20]. They demonstrated phosphate-based glass fiber reinforced composites could be a candidate for bone fracture fixation devices. Park et al. investigated tensile, four-point bending, fatigue tests and microscopic observations of a composite fixation plate made of a glass/polypropylene (Twintex) [21]. They found appropriate forming conditions for molding and carried out a water absorption test to study the performance of composite fixation plates under a simulated human body condition. They found water absorption has a little effect on the flexural stiffness and strength of this composite fixation plate and suggested that GF/PP can be used to construct a fixation plate under body fluid condition. Also, Liesmaki et al. investigated three-point and four-point bending of the composite fixation plate using experimental and numerical methods [22]. In their study, they used plates made with Bisphenolaglycidyl methacrylate (BisGMA)/Triethylene glycol dimethacrylate TEGDMA matrix reinforced with different types of glass fiber. Also, they compared the results of these plates with CF/PEEK

and stainless steel plates. They found that unidirectional glass fiber is a suitable candidate for reinforcing BisGMA in this kind of fixation devices.

It is clear that there are very materials that satisfy all the mechanical properties exhibited by bone. Hence, different researches used various types of composite materials to fabricate composite fracture fixation plates but the proposed materials more or less have disadvantages in biological or mechanical aspects. Therefore, bone fracture fixation devices still need further development to produce a fixation plate with appropriate mechanical properties. Since GF/PP composite material are biocompatible with the minimum negative effect on the body health [5], the objective of the current study is to evaluate mechanical properties of GF/PP composites plates. The mechanical properties of general importance to biomaterials development include Young's modulus, ultimate tensile strength and fracture toughness. This study aims to investigate the mechanical properties of the GF/PP composites fracture fixation plate, including tensile, compression, flexural, shear and impact resistance. For the experimental evaluation, three different fiber types; PP/Short Chopped Glass Fiber (PPSCGF), PP/Long Glass Fiber (PPLGF) and PP/Long Glass Fiber Yarn(PPLGFY) have been used. Also, manufacturing processes, microscopic observations and damage mechanisms have been closely assessed. Furthermore, the results have been compared with previous researches.

2. Materials and Experimental Methods

2.1. Materials and Design

The literature has reported several challenges in using thermoplastic polymers as matrix materials [5 and 21]. The challenges are mainly due to that high viscosity and the difficulty in achieving fiber alignment in continuous fibers within the matrix. Hence, the aim of this study is to produce GF/PP fracture fixationplates that contain different types of glass fiberand finding

an appropriate range of longitudinal Young's modulus of the fixation plate. Three different types of glass fibers were used for fabrication of the samples as following:

- PP/Short Chopped Glass Fiber (PPSCGF)
- PP/Long Glass Fiber (PPLGF)
- PP/Long Glass Fiber Yarn(PPLGFY)

Plate geometry was designed considering an anatomical tibia model. The plate designed for a tibia middle shaft fracture with dimensions of 110 mm length, 25 mm width and 5.5 mm thickness. It has been reported that the position of screws next to the fracture site plays an important role in the stiffness of the fixation plate structure. It also suggested that not less than three screws should be used in each side of the bone fragment [23]. Hence, the fixation plate model designed with six screw positions is suggested as shown in figure 1.

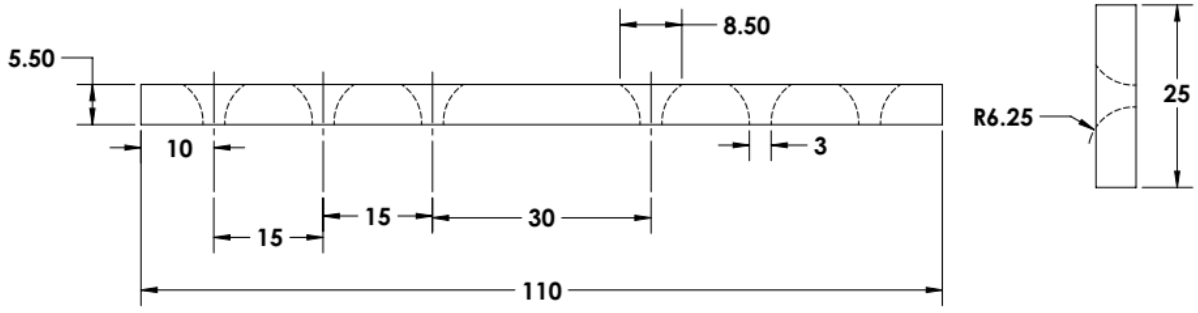

Figure 1. Geometry of composite fixation plate (All dimensions in mm).

2.2. Hot Press Manufacturing Process

Prepregs of unidirectional long fibers and random short fibers were used to fabricate the fixation plates and the mechanical performances of reinforced composite fracture plates were evaluated accordingly. Hence, the PPSCGF granules and PPLGFprepreg sheets(20 layers of unidirectional fiber sheets) with the density of $1.04 \pm 0.01\ \mathrm{g/cm^3}$ and $1.27 \pm 0.01\ \mathrm{g/cm^3}$and the volume fractions of 15% and 30%, respectively were used to manufacture two types of fixation plates.

It has been recognized that drilling a hole after the composite has been fabricated, can reduce its load-carrying capacity to a remarkable extent due to the breakage of fiber continuity. Hence, to create screw holes in the fixation plate without disconnecting the continuity of the fibers, a stainless-steel mold die with six pins were used (Figure 2). The mold die was put into a hot-press machine and it was heated to 230°C for 10 min to avoid relaxation of the reinforcing polymer fibers. When the desired temperature and compression pressure were achieved, the mold was held under constant pressure for 20 minutes (Figure 3). Afterward, the mold was gradually cooled to the room temperature and finally, the compressed composite fixation plate was ejected from the mold die.

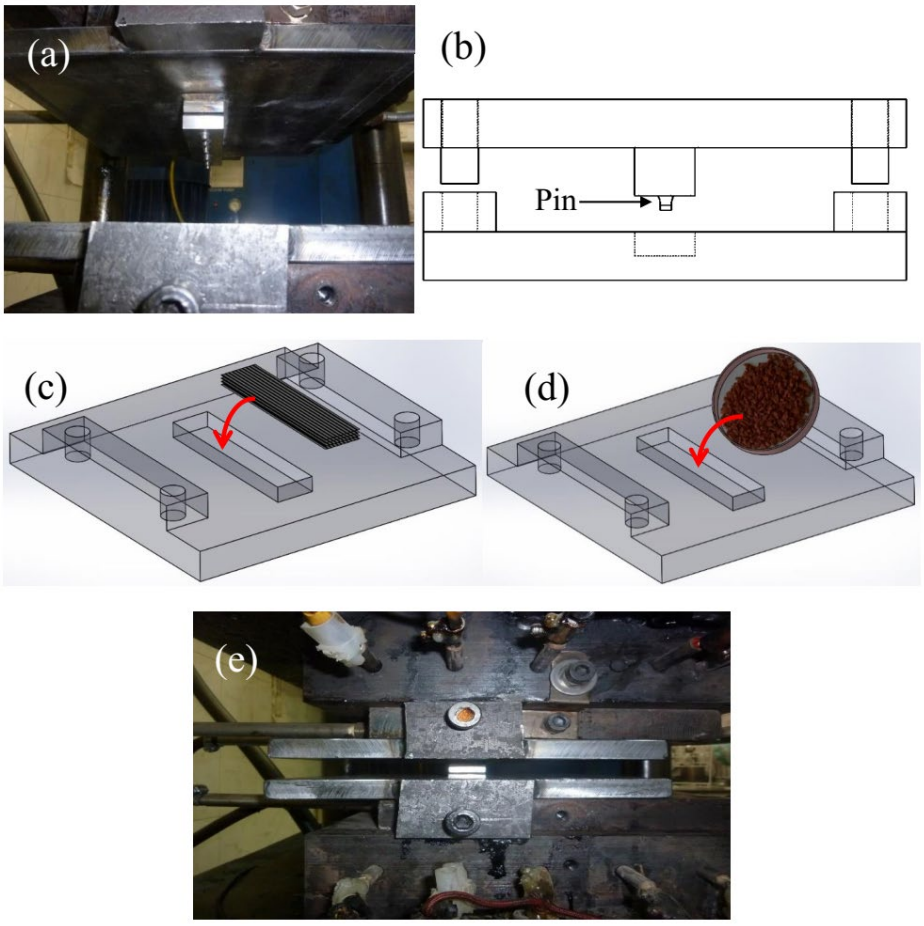

Figure 2. Specimens preparation by thermoforming and insertion way of PPSCGF granules and prepreg sheets of PPLGF in mold, (a) preheat the mold, (b) schematic drawing of molding, (c) insertion of prepreg sheets, (d) insertion of granules, (e) applied pressure and cooled mold.

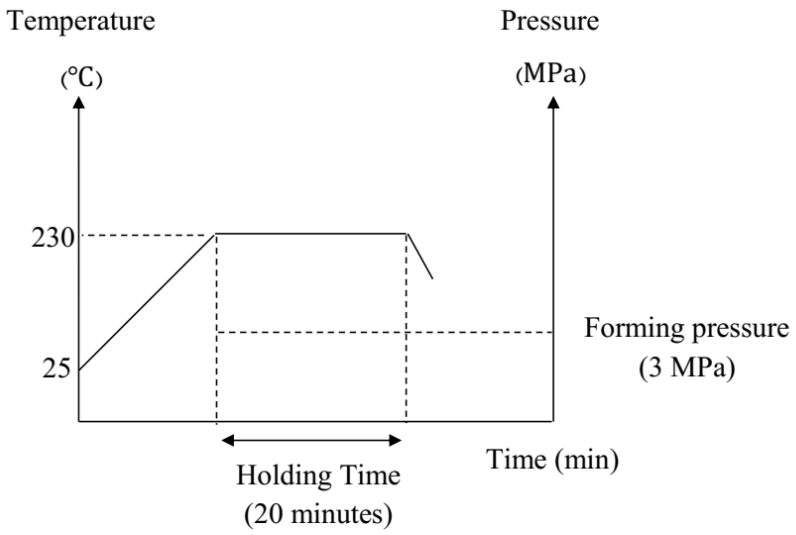

Figure 3. Forming pressure-temperature cycle of specimen preparation.

2.3. 3D Print Manufacturing Process

Three-dimensional (3D) printing is an additive manufacturing process to construct 3D objects to form digital models. The 3D printing technique is a rapidly growing trend in bioengineering [24]. Hence, in this study used the 3D printing method to produce the PPLGFYfixation plate. The computer model was generated as a G-code file using slic3r V1.3.0 software applicable for a 3D printing machine. The PP filament initially placed in a heating jacket to heat up the sample to 220°C, then it was extruded through the nozzle [24 and 25]. The schematic of a fused deposition modeling (FDM) process is shown in figure 4. As it is illustrated, the input fiber yarn was held by a pulley and then it was released into the nozzle and was embedded into a molten area. The inner diameter of the nozzle was 0.4 mm. The thickness of each layer and printing speed were 0.22 mm and 5 mm/sec, respectively. Also, glass fiber yarn was used with a mass per length of about 0.1 g/m and a volume fraction of 15%. Furthermore, PP was used in the form of filament with a diameter of 1.75 mm.

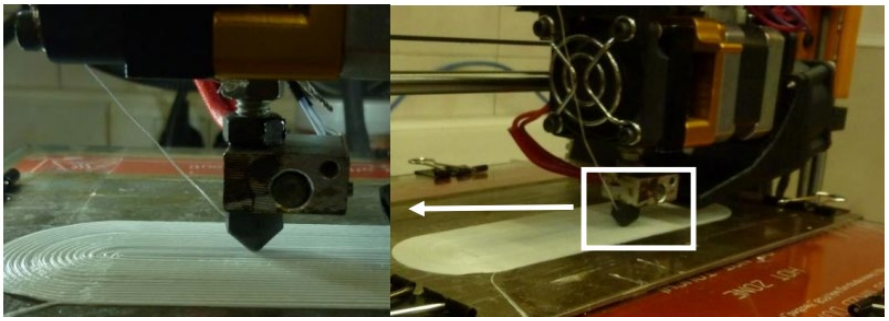

(a)

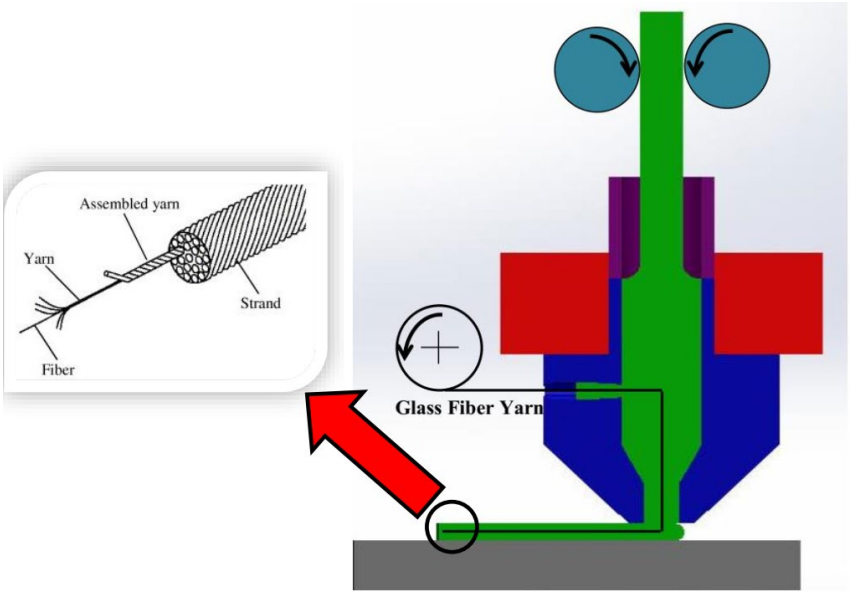

(b)

Figure 4. Simultaneous impregnation systems; (a) 3D printing manufacturing, and (b) The schematic of the FDM process.

After completion of the manufacturing process, all sharp edges were removed. The fabricated composite fixation plate samples are shown in figure 5.

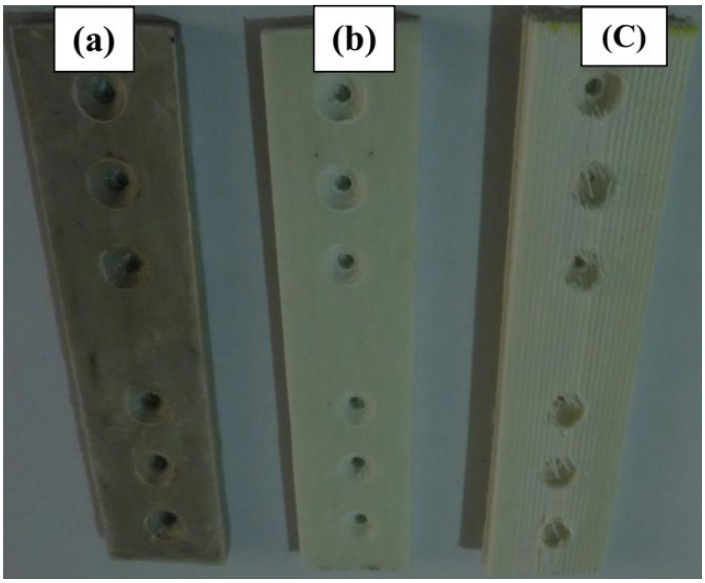

Figure 5. Fabricated composite fixation plates; (a) PPSCGF, (b) PPLGF and (c) PPLGFY.

2.4. Microscopic Investigations

The cross-section of all three composite fixation plate samples was observed utilizing a scanning electron microscope (SEM) at room temperature. SEM analysis with field emission gun and accelerating voltage of 5 kV was used to collect 800X magnified images from the composite specimens.

2.5. Tensile, Shear and Compression Testing

Tensile test samples were prepared according to ASTM D3039 [26] for each type of GF/PP composites, and ASTM D638 [27] for neat PP. For shear and compression testing of the specimens, ASTM D3518 [28] and ASTM D3410 [29] were followed respectively and a support jig was used as advised. The experiments were conducted on a tester machine (5500 series, Instron Co., the UK with 20 kN load cell) with a loading rate of 2 mm/min at room temperature. The strain field vector was monitored through the digital image correlation (DIC) technique (Figure 6). The modulus of elasticity and shear modulus, i.e. slope of the stress-strain curve, was obtained by applying linear regression to the linear domain of the experimental stress-strain curve [26-29]. Furthermore, the ultimate tensile, shear and compression strength and strain were measured prior to the failure. Then, the mean value and standard deviation of the obtained results were calculated.

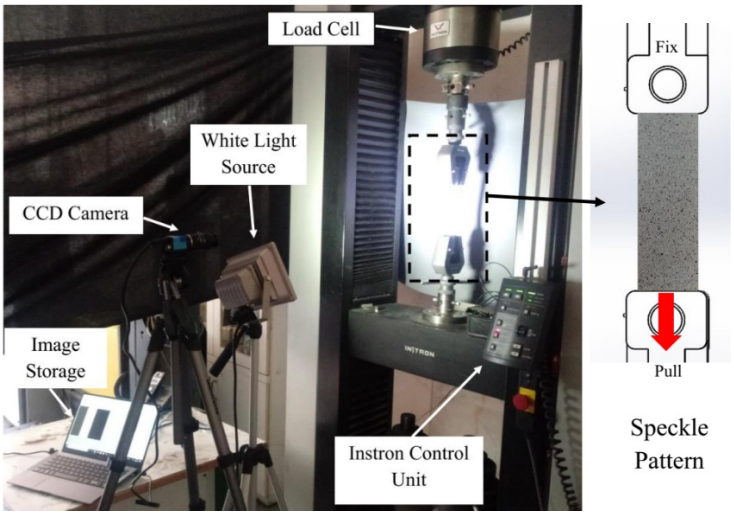

Figure 6. Tensile, shear and compression tests setup.

2.6. Flexural Testing

From the practical point of view, the bending behavior of a fixation plate plays an important role to quantify the mechanical properties of the samples. The flexural test was performed considering of flexural stiffness and modulus, and maximum bending moment. In this study, a 5500 series-Instron universal test machine was used to conduct the four-point bending test of fixation plates at room temperature in accordance with the procedures of ASTM D7264 [30]. The test setup is depicted in figure 7.

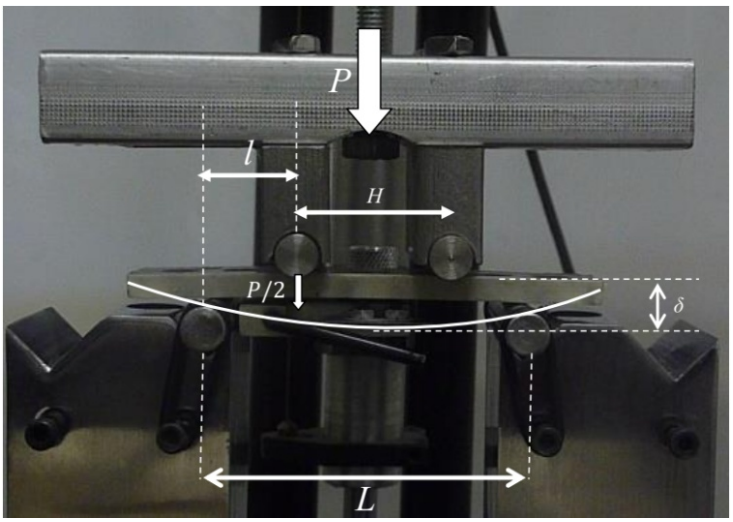

Figure 7. Four-point bending test setup.

Until the specimen failure, the load was increased and the equivalent flexural modulus (EFM) was calculated using the equations associated with standard flat specimens. Using the load-deflection and stress-strain curves, the bending moment (M), bending angulation (θ), bending stiffness (BS), ultimate bending stress (σ_U^B) and bending elastic modulus were derived via the classical beam theory following equations [21]:

$$M = \frac{P}{2} l \tag{1}$$

$$\theta = \tan^{-1}\left(\frac{\delta}{l}\right) \times \frac{180}{\pi} \tag{2}$$

$$BS = \frac{M}{\theta} \tag{3}$$

$$\sigma_U^B = \frac{M_{max}\bar{y}}{I} \tag{4}$$

Where$P$ is the applied load, l is the length between the outer and inner rollers, δ is the deflection at the center of the fixation plate, $\bar{y}$ is the position of the neutral axis, and I is the second moment of inertia of the cross-section in the x-axis.

2.7. CharpyImpact Testing

Impact testing of theGF/PP composite samples was carried out by an instrumented Charpy impact test. The Charpy pendulum is a simple method for obtaining energy absorption and dissipation in test samples [31]. Test specimens were prepared with a mid-point notch as shown in figure 8-a. The specimen was supported in a horizontal plane and impacted by the swinging pendulum directly opposite the notch (Figure 8-b). The specimen geometry was according to the ASTM D6110 [31], and the impact resistance (kJ/m^2) was calculated by dividing the recorded absorbed impact energy into the cross-sectional area of the specimen.

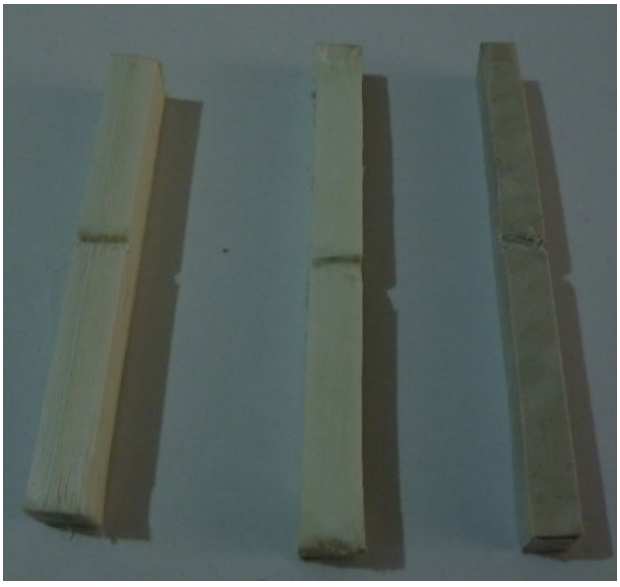

(a)

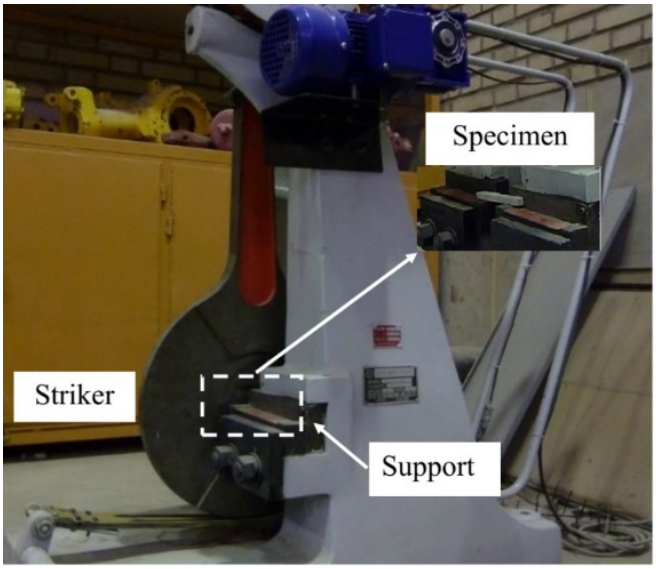

(b)

Figure 8. (a) Charpy test specimens, and (b) Charpy test setup.

3. Results and Discussion

3.1. General Findings

The mass density less than 1.5 g/cm3 (1.04 ± 0.01, 1.27 ± 0.01 and 0.49 ± 0.01 g/cm3 density for the PPSCGF, PPLGF and PPLGFY, respectively) can be achieved by employing certain manufacturing methods. Due to the formation of voids in the manufacturing process of the PPLGFY, the density of this sample is much less than the samples made by heat-compressing method. These voids are created between rasters and layers, most often inevitably. Also, the lower percentage of glass fibers used in the PPLGFY compared to the PPLGF intensifies the difference in the density values. Generally, density values of all the fabricated composite fixation plates are much smaller than the stainless steel plate density (7.8 g/cm3). Hence, the composite fixation plates are much lighter than the stainless steel plate (Figure 9).

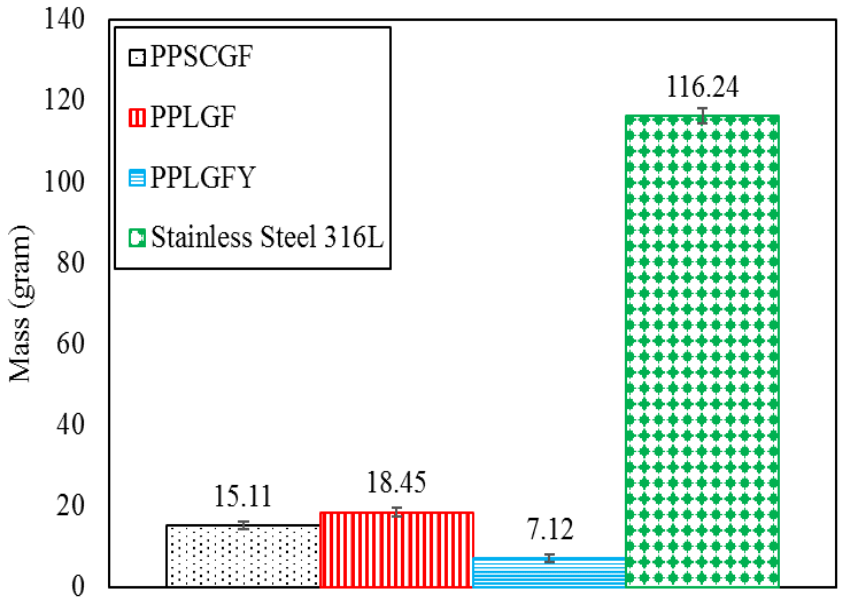

Figure 9. Mass comparison of fabricated composite fixation plates similar geometry to Stainless Steel 316Lfixation plate.

Also, it has been reported that polymeric composite materials are substantially higher fatigue resistance than stainless steel, which gives these an ability to be suitable candidates for sustaining cyclic loads of the lower limbs during daily activities [21]. Furthermore, at room temperature(30℃), the water content and the degradation rates of the bending stiffness and flexural strength of the polypropylene/glassin body fluid were very low and also the glass fibers can be reduced the water absorption rate [21]. Hence, based on the abovementioned advantages, it may be concluded that the GF/PP composites are good candidates for a long-term orthopedic implant in the human body.

3.2. SEM Observations

The electron microscope images of specimens were used to compare the applied methods in the production of the fixation plate and investigate the fiber angle, its orientation and quality of the interfacial bonding between the fibers and matrix. The diameter of the observed glass fibers varied between 5-20 μm. The SEM micrographs of the all three types of composites samples, as shown in figure 10, clearly indicated that fibers in the core layer were preferentially parallel to the X-direction and are hence attached to the PP matrix. As shown in this figure, the

adhesion and bonding between the fibers and the polymer appears desirable. The micro-fibers compaction is also noticeable in this figure. The fiber has been covered with a thin layer by the matrix linking the fiber surface to the matrix. This linking causes better stress transfer and enhances its flexural property. In addition, more uniformity was observed in the fabricated sample using PPSCGF (Figure 10-a) due to the shortness of the fibers. On the other hand, the PPLGF composite contains gaps and voids around the fibers due to the higher percentage of fibers rather than the two other composite samples, as illustrated in figure 10-b. The voids in the composite structure may exist either inside the matrix or at the interface. Those voids lying at the interface play a more important role in reducing mechanical properties than those inside the matrix. Unexpected voids generation in the composite structure depends on the manufacturing parameters such as temperature, time, and an intrinsic viscosity of the thermoplastic polymer and also fiber volume fraction. Furthermore, the size and number of voids are affected by the topographic surface of fibers. From microstructure point of view, increasing the pre-heating time and forming pressure increases the fiber concentration in the composite and reduces the voids around the fibers.

Since there are strong forces acting on the polymer melt in Y and Z directions in a hot press and 3D printing methods, long fibers could not deviate from the X-direction (Figures 10-b and 10-c). As a result, the micrographs reveal that almost all fibers laid parallel. Due to high viscosity of the PP, the weakness in fused deposition modeling and the structure of the braided fibers caused that PPLGFY composite samples suffer from a poor impregnation compared to hot press samples. Thus, gaps and voids around the fibers (i.e. interface of fibers and polymer matrix) can be seen in the final products (Figure 10-c) and led to the growth of cracks during axial loading.

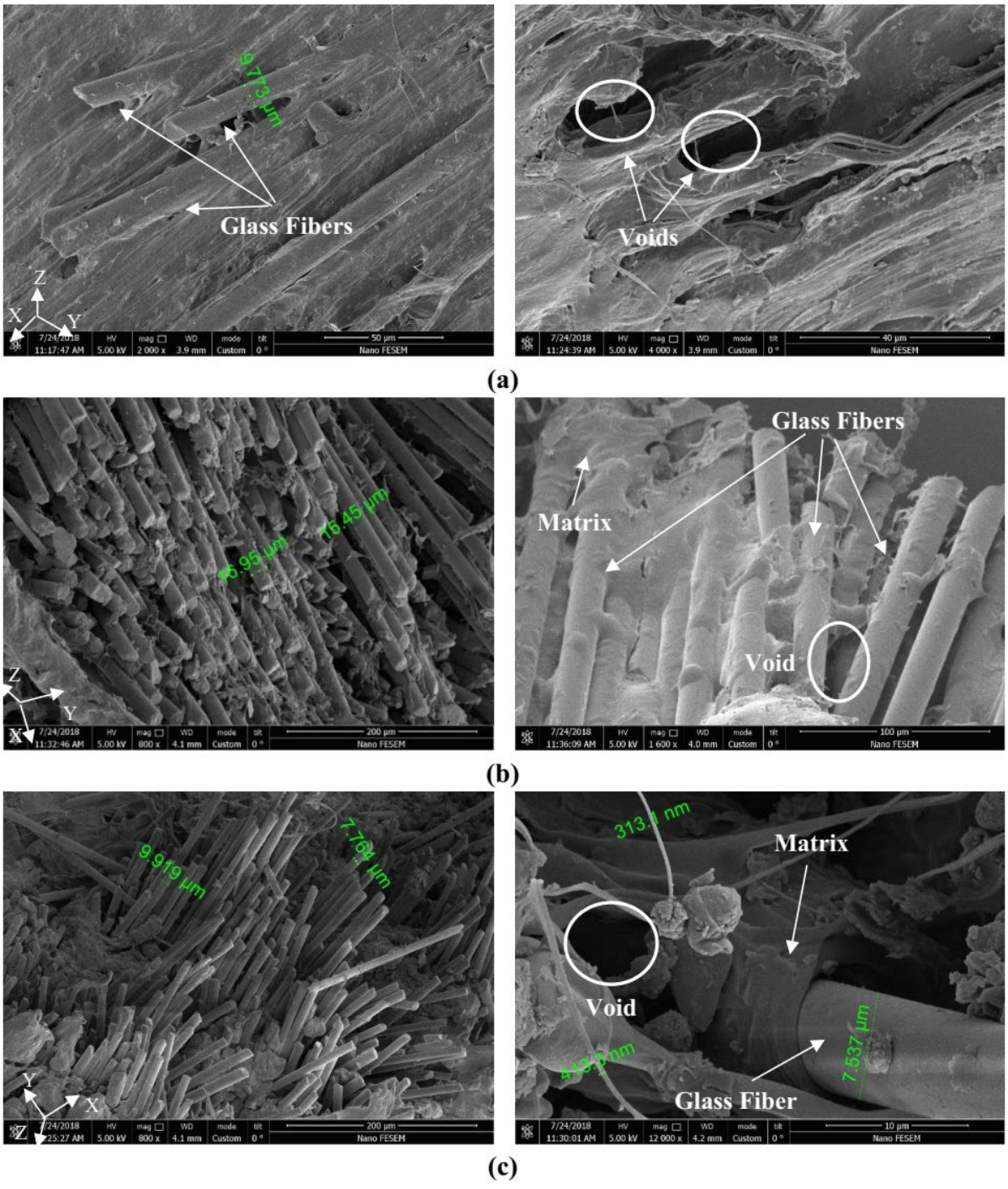

Figure 10. SEM micrographs of the; (a) PPSCGF, (b) PPLGF and (c) PPLGFY.

Generally, modulus, strength and other properties depend on the fiber content, orientation and quality of the interfacial bonding between the fibers and matrix. The obtained results (see Table 1) indicate that the composite consisted of the largest amount of sizing and higher fiber volume fraction (PPLGF) has the best tensile, compression, shear, flexural and impact strength

performances. It is also obvious that fiber-fiber and fiber-matrix friction contributions should be also taken into account as the fiber type with the highest sizing amount, thus the highest interface strength was expected. As such, the interfacial bonding between the glass fibers and the PP were clearly affected by the friction forces which are closely related to the amount of sizing on the fibers surface.

The main parameters in FDM process including nozzle temperature, envelope temperature, layer height, nozzle diameter, extrusion width, air gap, part or rater orientation, raster angle, filling pattern, and filling percentage. Poor impregnation, existence of voids and low strength are the main weaknesses of the FDM 3D printed sample compared to the manufactured ones by heat-compressing process. These characteristic may be related to both of inherent weakness of thermoplastic materials and poor adhesion between the each layer. Consequently, lower tensile and compressive properties, and impact resistance of the 3D printed sample are expected. Also, the nature of the FDM process creates residual stress in the printed parts, which may result in warpage and delamination of the specimens.

3.3. Tensile Test

The elasticity modulus of fixation plate material should be selected to ensure a more uniform distribution of stress at the fixation plate and to minimize the relative movement at plate-bone interfacial contact. Figure 11 illustrates the stress-strain curves of composite samples and neat PP. A comparative diagram of the axial Young's modulus in the longitudinal direction of the fiber shown in figure 12. The strength and modulus values were 30-400 MPa and 2.35-20.10 GPa, respectively for composites in room temperature and dry conditions, which were in the range of cortical bone (50-150 MPa, 7-30 GPa [32]).

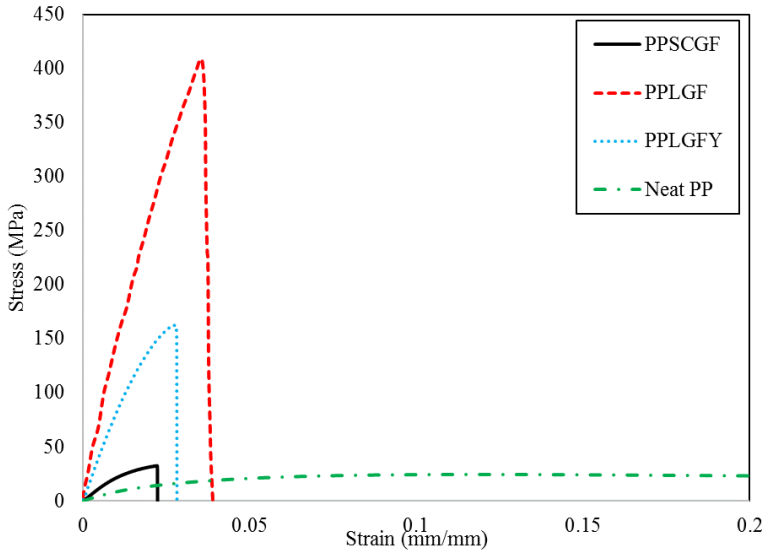

Figure11. Comparison of specimen stress–strain curves through the fiber direction.

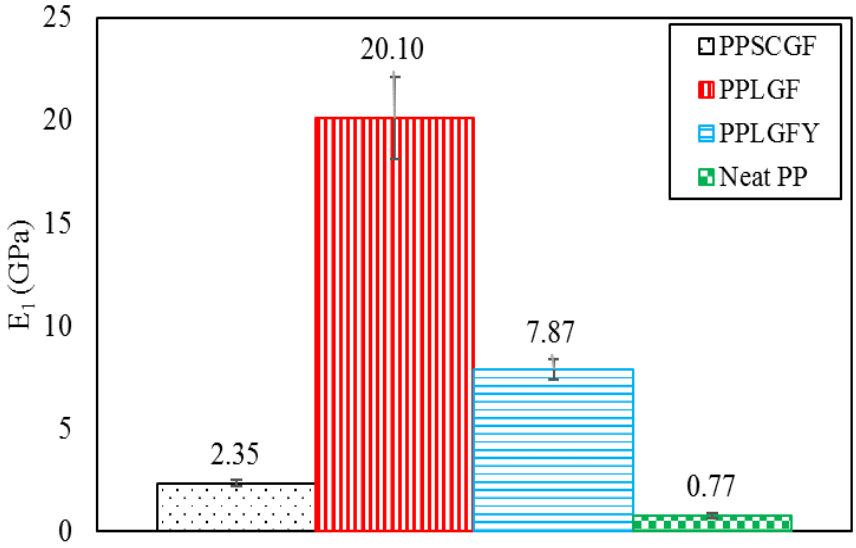

Figure12. Comparison of Elastic modulus through the fiber direction.

The highest and lowest tensile modulus belong to PPLGF and PPSCGF composites with 30% and 15% glass fibers volume fractions, respectively. It has been observed that short chopped fibers are not acting as efficient as long continuous fibers due to difficulties in controlling their orientation and the lower ratio of fiber length to carry full axial stress. As a result, a composite with long fibers oriented in the direction of maximum stress would have superior properties compared with randomly distributed short fiber composite. In the tensile testing of the specimens, after reaching the peak value at the failure point, there was a sudden drop of load for all composite samples. PPLGF and PPLGFY specimens showed edge delamination or long

splitting in their glass fibers on both sides of the fracture zone. In addition, the initiation of cracks in matrix and fiber tearing occurred. Despite this fact that neat PP exhibits a perfectly plastic behavior after the linear elastic region, sudden failure occurred to all types of produced composites regarding their brittle manner.

3.4. Shear Test

The mean results for shear modulus and strength of different specimens with standard deviations are summarized in Table 1 in which the shear strength is calculated from the ultimate load to the onset of delamination and crack initiation. The values of the in-plane shear modulus (G_{12}) and strength (τ_{12}) are the more important than other directions for the fixation plate application. They have been determined from stress-strain curves and their values were 1.42-0.25 GPa and 40-10 MPa, respectively in room temperature and dry conditions.

Due to the poor adhesion of the PPLGFY, delamination between the individual plies manifests itself at low loads, and results in a rotation of the fibers in the loading direction more than other composites. In composite with better fiber-matrix adhesion (PPLGF), only little interplay failure occurs; therefore, extensive fiber rotation is prevented and the failure process is more local.

3.5. Compression Test

The compression test results are summarized in Table 1. The longitudinal ultimate strength was measured just before the occurrence of the buckling. It was 45 ± 5, 30 ± 5, and 70 ± 5 MPa for PPSCGF, PPLGFY and PPLGF samples, respectively (Tables 1). They show an approximate 2.25, 1.5 and 3.5 times increase in longitudinal compressive strength for the PPSCGF, PPLGFY and PPLGF composites compared to the neat PP, respectively. A combination of longitudinal splitting and fiber buckling as the predominant failure modes was observed for PPLGFY and PPLGF specimens tested. During compressive testing, the plates

were observed to delaminate significantly, in parallel to the long axis, starting from the point where the plate makes a contact with the mechanical tester's clamps. Compressive properties of the composite fibers were expected to increase with the increasing glass fiber content within the structure due to glass fibers. In general, the matrix and interface mode failures occurred compared to the fiber failure mode in specimens.

3.6. Flexural Test

The main purpose of this study was to develop glass fiber-reinforced composites with flexural elastic modulus in the range of that for human cortical bone. The comparative diagrams (Figures 13-16) represent the bending moment–angulation, flexural stiffness, flexural elastic modulus and flexural strength of all four fixation plate models tested at room temperature and dry conditions. Four-point bending test results reveal a significant improvement in bending modulus and strength by increasing fiber percentage compared with the neat PP fixation plate. The curves of bending moment versus bending angulation for all produced fixation plates are illustrated in figure 13. For a bending angle value of 7 to 25 degrees, the maximum bending moments were attained. According to the trend of the PPSCGF and PPLGF diagrams, it is evident that the bending moment increased up to the maximum moment and suddenly dropped when the initial fracture became visible at the tension side, especially in the vicinity of supported areas. In PPSCGF, the bending behavior is plastic and eventually yields in a brittle fracture. While the PPLGF exhibits completely different behavior. No significant decrease in flexural load is observed and still capable of load-bearing while its interlayers separated due to compression and tension in surfaces. The PPLGFY bending curve, the same as neat PP presented ductile behavior. This ductile behavior can be explained by the observation of specimens after the test, as the fracture is not occurring in the flexural test.

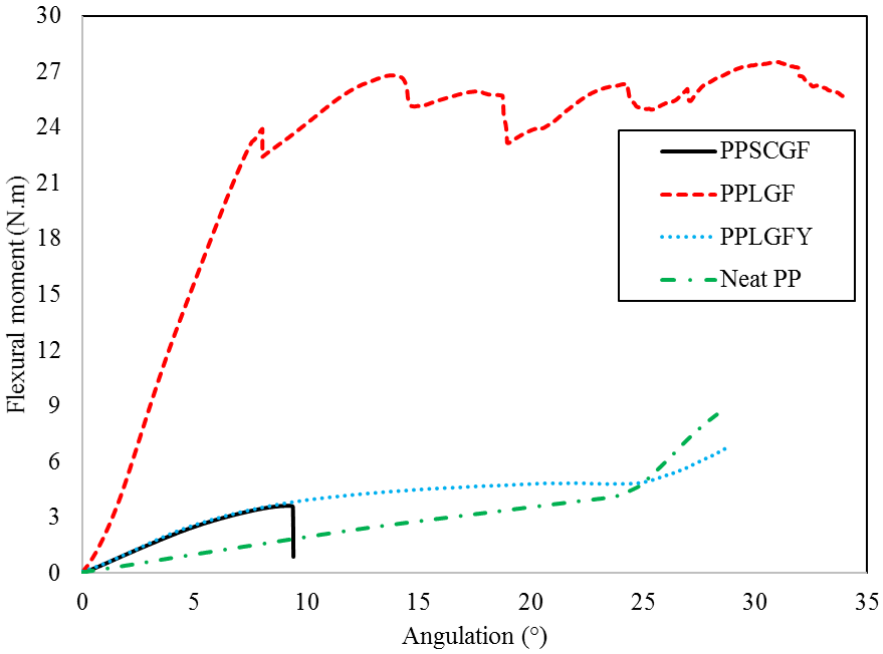

Figure13. Comparison of fixation plates bending moment-angulation curves.

The flexural stiffness, modulus and strength values are shown in figures 14-16. Their values are 0.44-3.274 N. m/°, 2.1-16.2 GPa and 27-185 MPa, respectively for composite specimens. Based on the findings, the highest reported modulus value is still below the flexural modulus value of the cortical bone (12-17 GPa [33]). This means that flexible GF/PP plates can significantly reduce stress shielding compared with metallic plates. Although, they have provided the desired stiffness for the initial phase of healing. In addition, they cause interfragmentary strain about 2 to 10% in the second phase of healing (indirect healing) at the callus zone, which can promote the healing process [34]. Therefore, the proposed composite fixation plates can be recommended as a proper candidate for orthopedic applications. Furthermore, their flexibility allows a good match with an unstable or multi fractured bone. Figures 14-16 demonstrate that the unidirectional PPLGF fixation plate has the maximum flexural stiffness, modulus and strength among all tested composite plates. However, poor transverse load capacity, inter-laminar damage and delamination of this could be issues. Consequently, the stresses near the screw holes can initiate crack which may split the sample along the axial direction.

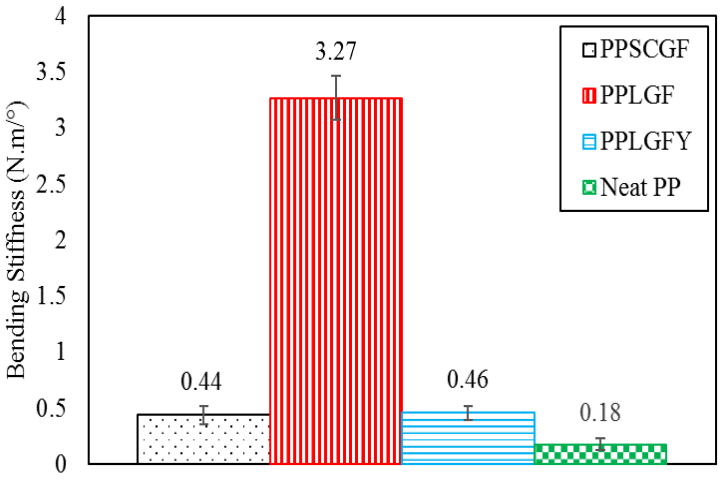

Figure14. Comparison of flexural stiffness.

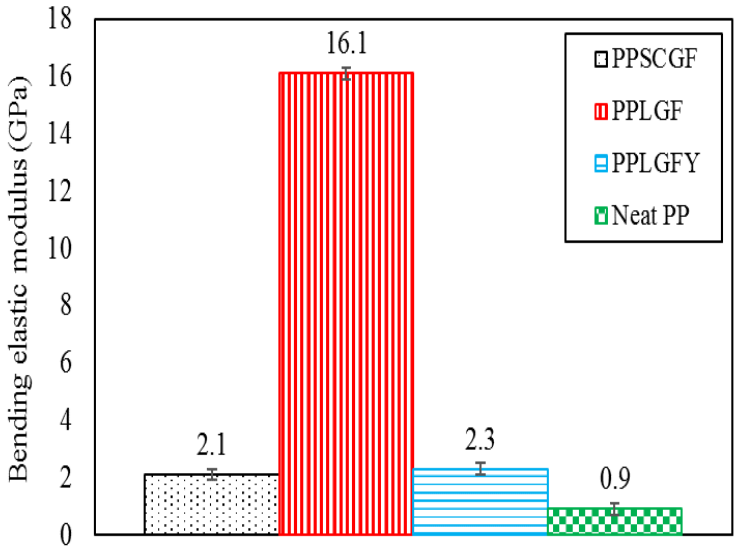

Figure15. Comparison of flexural elastic modulus.

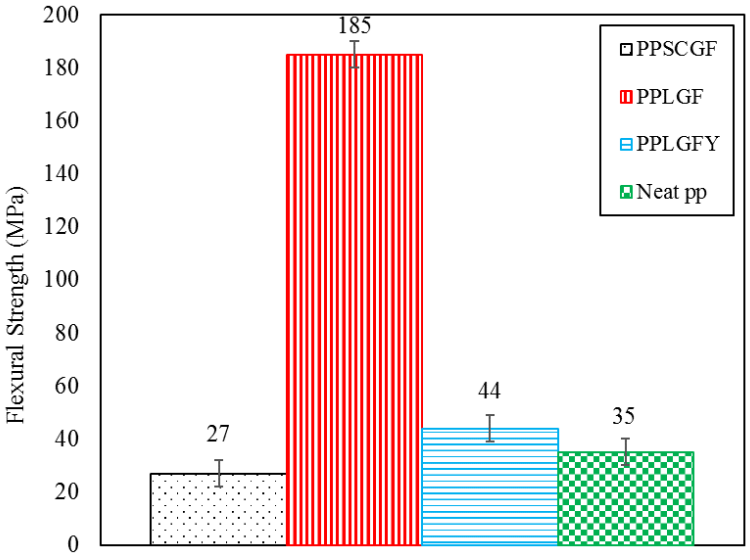

Figure16. Comparison of flexural strength.

Damage patterns identification clarified delamination, debonding, crack opening and fiber pullout as the major sources of damage [35]. These could be evidenced by the formation of micro void spaces within the composite. As it can be seen in figure 17, the delamination and fractures of the load-bearing area in the fixation plate can be considered as predominant failure modes. On the other hand, the failures occurred at the outer surfaces due to matrix cracking in the PPSCGF (Figure 17-a). And fiber breakage along and perpendicular to the compressed surfaces, which was followed by progressive delamination of the GF/PP prepreg plies in PPLGF (Figure 17-b). Also, the delamination was observed in the compressive side of the specimen beneath the loading points. Although the failure didn't happen in a brittle trend, the failure may be represented in the oscillated dropping region in the load-deflection curve. Generally, the tension failure causes a separation in the outer layers of the PPLGF fixation plate, which continues to bend and redistribute the stress levels through the cross-section in compression failure. Also, cracks initiated and propagated around the third screw hole beneath the loading points.

The 3D print fixation plate presents plastic behavior and no fracture was observed during the test (Figure 17-c). Bending load which may be the consequence of PP existence in conjunction with the considerable tensile strength of yarn glass fibers.

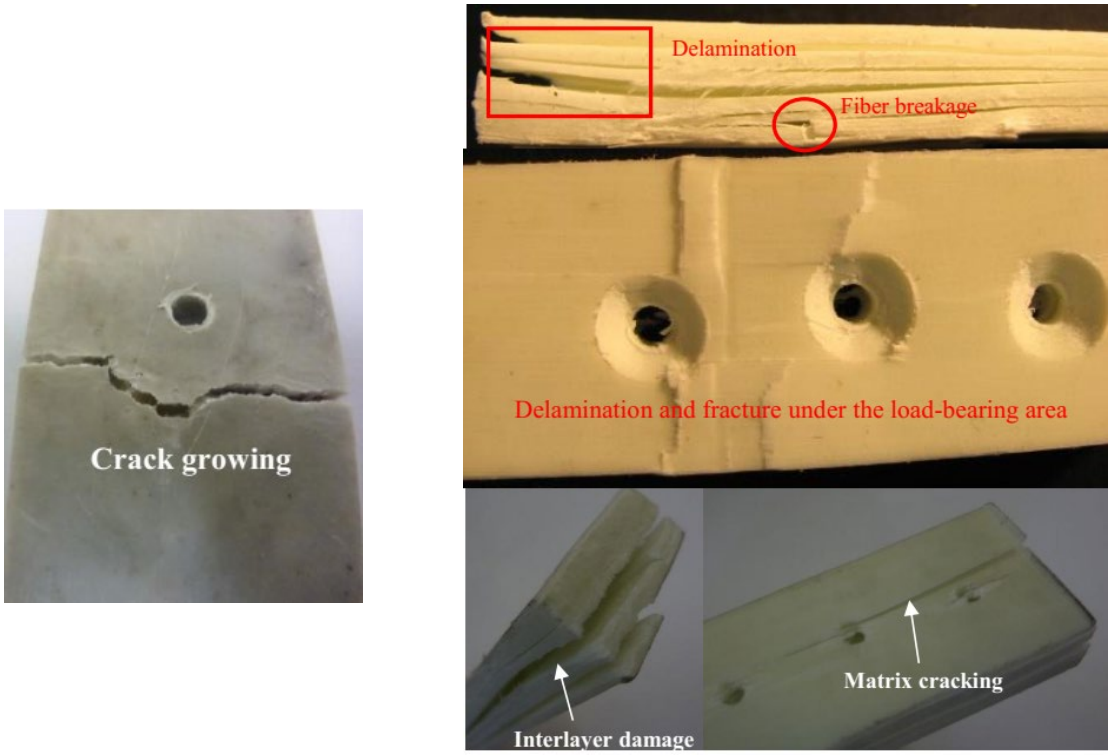

Figure17. Bending test specimens; (a) PPSCGF, (b) PPLGF and (c) PPLGFY.

3.7. CharpyImpact Test

In general, fiber characteristics such as type, orientation and volume fraction play an important role in the impact properties of glass fiber reinforced PP composites. Furthermore, the impact response of such composites is strongly affected by the fibers-matrix interfacial bond strength in unidirectional laminates [36]. As a result, the higher volume fraction of fibers in PPLGF and acceptable fiber/matrix bonding result in higher impact strength compared to other composites (Figure 18). The PPLGF and PPLGFY composites shown a remarkable impact strength of 162 ± 5 kJ/m^2 and 68 ± 5 kJ/m^2, respectively, which were about 7 and 3 times larger than the

PPSCGF. It seems that the PPLGF impact strength can provide sufficient protection against external impacts for the human bones.

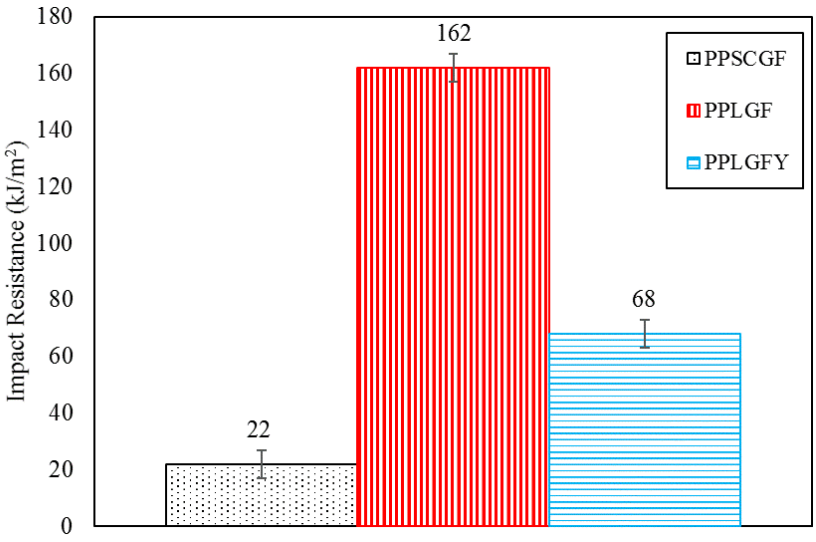

Figure18. Comparison of impact resistance.

(a)

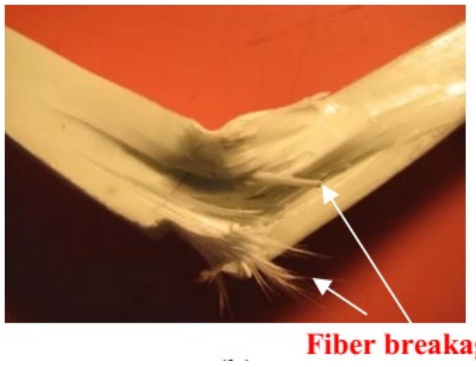

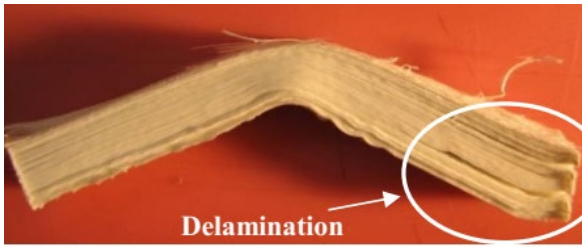

(b) (c)

Figure19. Charpy test specimens; (a) PPSCGF, (b) PPLGF and (c) PPLGFY.

As it is illustrated in figure19-a, an abrupt fracture occurs in the PPSCGF sample. However, the failure mechanism in other composite types is different from the PPSCGF and may be related to the type of glass fibers. In fact, deterioration trigger mechanism in PPLGFY and PPLGF is due to interlayer damage and crack growing in fibers and matrix, respectively, and

finally fracture occurred in the form of delamination and fiber breakage (Figures19-b and 19-c).

3.8. Summary of Obtained Mechanical Properties

In this study, in addition to the results of tests mentioned in the sections 3.3-3.5, tensile, compression and shear tests in two other directions have been also carried out. Furthermore, the density of specimens was measured using the Archimedes principle (ASTM D792 [37]), which involved the immersion of a known weight of each composite into a lower density solvent. Table 1 illustrates various mechanical properties including density, Young's modulus, tensile and compressive strength, shear modulus, shear strength, Poisson's ratio, flexural modulus and strength and impact resistance of the tested samples. In order to identify the mechanical properties of specimens, six samples were replicated and the mean values and the standard deviations (SD) were calculated. To simplify the presentation of the results, characteristic curves and graphs of each set with a close value to the average results were selected.

Table 1.Obtained values of mechanical properties (1, 2 and 3 are the principal directions).

Properties	PPSCGF	PPLGF	PPLGFY	Neat PP
$\rho(kg/m^3)$	1040 ± 10	1270 ± 10	490 ± 10	946 ± 5
$E_1(GPa)$	2.35 ± 0.15	20.10 ± 2	7.87 ± 0.5	0.77 ± 0.1
$E_2(GPa)$		4.20 ± 0.3	1.00 ± 0.2	
$E_3(GPa)$		4.20 ± 0.3	1.00 ± 0.2	
$\sigma_{U1}^{T}(MPa)$	30 ± 5	400 ± 30	150 ± 20	20 ± 5
$\sigma_{U2}^{T}(MPa)$		20 ± 2	10 ± 1	
$\sigma_{U3}^{T}(MPa)$		20 ± 2	10 ± 1	
$\sigma_{U1}^{C}(MPa)$	45 ± 5	70 ± 5	30 ± 5	20 ± 5
$\sigma_{U2}^{C}(MPa)$		50 ± 5	15 ± 5	
$\sigma_{U3}^{C}(MPa)$		50 ± 5	15 ± 5	
$G_{12}(GPa)$	0.8 ± 0.1	1.42 ± 0.2	1.15 ± 0.2	0.25 ± 0.1
$G_{13}(GPa)$		1.33 ± 0.2	1.1 ± 0.2	

$G_{23}(GPa)$		1.33 ± 0.2	1.1 ± 0.2	
$\tau_{12}(MPa)$	20 ± 5	40 ± 2	20 ± 2	10 ± 5
$\tau_{13}(MPa)$		30 ± 2	10 ± 2	
$\tau_{23}(MPa)$		30 ± 2	10 ± 2	
ν_{12}	0.35 ± 0.05	0.15 ± 0.05	0.25 ± 0.05	0.45 ± 0.05
ν_{13}		0.10 ± 0.05	0.15 ± 0.05	
ν_{23}		0.10 ± 0.05	0.15 ± 0.05	
$E_B(GPa)$	2.1 ± 0.2	16.2 ± 0.2	2.3 ± 0.2	0.9 ± 0.2
$\sigma_U^B(MPa)$	27 ± 5	185 ± 5	44 ± 5	35 ± 5
$IR(kJ/m^2)$	22 ± 5	162 ± 5	68 ± 5	$-$

The written values are the mean value and the standard deviation (SD) of the obtained measurements from the properties tests.

3.9. Comparison to Previous Studies

Mechanical investigations mainly focused on macroscopic properties, strength and Young's modulus, in some cases load-displacement curves and fracture images were presented. Hence, the results of previous studies on the mechanical properties of reinforced composites used as flexible orthopedic fixation to facilitate the replacement of traditional metallic plates were summarized and compared with the results obtained in the current study (Table 2). There are some differences between the results of the current study and the literature due to different fiber and matrix constituent, fiber orientation, dissimilar fiber or matrix volume fraction and various manufacturing methods. However, the presented mechanical properties of the proposed GF/PP composites were within the reported range in previous studies.

Table 2. Comparison of mechanical properties of the current GF/PPcomposites to previous studies.

Composite	$E(GPa)$	$E_B(GPa)$	$\sigma_U^T(MPa)$	$\sigma_U^B(MPa)$	$IR(kJ/m^2)$	Ref
PPSCGF	2.35	2.1	30	27	22	Present study
PPLGF	20.10	16.2	400	185	162	Present study
PPLGFY	7.87	2.3	150	44	68	Present study
Neat PP	0.77	0.9	20	35	-	Present study
Kenaf/PLA	-	3-14	-	40-100	20-60	[12]
Hap/PLLA	2.5-4.2	-	10-70	-	-	[13]
MAWs/PLA			46-108	88-190	5-150	[14]
Bioglass/PCL	-	8-18	-	120-200	-	[18]
PG/ methacrylate-modified oligolactide	15-20	15-20	80-220	100-200	-	[19]
PG/PLA	-	5-12	-	50-120	-	[20]
GF/PP(Twintex)	7.5-19	-	215-550	220-250	-	[21]
Flax/Epoxy	12.98-30	-	148.1-200	-	-	[38-40]
Glass/Flax/Epoxy	16.51-31.97	30.03-39.84	301.87-408.25	499.98-591.25	-	[41]
Carbon/Flax/Epoxy	41.7	57.4	399.8	510.6	-	[42]
UD CF/Epoxy	50-300	-	-	-	-	[43]
2D CF/Epoxy	20-30	-	-	-	-	[43]
3D CF/Epoxy	10-20	-	-	-	-	[43]
CF/Flax/Epoxy	5.09-6.48	14.41-23.84	172.4-288.3	85-160.42	-	[44]
Sisal/CF/Polyester	1.99-2.78	6.52-11.33	84.44-107.51	140.89-169.14	-	[45]
Glass/BisGMA/TEGDMA Resin (UF-BG)	-	17.0	-	802.0	-	[46]
Glass/BisGMA/TEGDMA Resin (UFS-BG)	-	15.3	-	602.0	-	[46]

Generally, according to literature, polymer matrices are divided into two categories; thermoset and thermoplastic and there are three prominent reinforcement methods in polymer-based fiber composite materials, i.e., (I) unidirectional fiber laminates, (II) discontinuous short and long

fibers and (III) textile fabrics (woven, knitted, braided and yarn fabrics) laminates. The types of fibers i.e. Carbon Fiber (CF), Glass Fiber (GF), Kenaf, Flax and Silk [5, 12, 18, 21, 41-47] were widely used in thermoset and thermoplastic matrix. Although due to the possible toxic may affect the human body and non-suitability to reshape at the time of surgery, the thermoset composites were not been suitable as an internal fixation device [5]. Also, thermoset polymers are not polymerized completely, which means some monomers still exist in the material after the polymerization [5]. Examples of thermosets, which utilized as biomaterials, are epoxy polymer and polymethylmethacrylate (PMMA) [5, 19, 38-44, 48-50]. On the other hand, the usage of thermoplastic polymers due to the ability of reshaping to the bone shape during the surgery by simply applying heat, is increasing [5]. Additional advantage of thermoplastic polymers is the greater fracture toughness compared to thermosets [5]. Another reasons for using thermoplastic polymers is to decrease composite manufacturing time, because thermoplastic polymers do not need chemical reaction time as the thermosets [5]. Examples of thermoplastics with biomedical applications are polyethylene (PE), polyetheretherketone (PEEK), polyacetal (PA), polyurethane (PU), polypropylene (PP), poly-L-lactic acid (PLLA), polylactic-co-glycolic acid (PLGA) and polylactic acid (PLA) [5, 12-14, 20, 21, 51-59].

4. Conclusion

GF/PP composites based on using three different fiber types (PPSCGF, PPLGF and PPLGFY) were introduced as a potential candidate for fixation plate application in this paper. The influence of glass fiber type, orientation and volume fraction and manufacturing process on the tensile, flexural, compression, shear and impact properties of the composite fixation plates was investigated. The obtained values of Young's modulus, tensile strength, flexural modulus, flexural strength and impact strength of specimens are 2.35-20.10 GPa, 30–400 MPa, 2.1-16.2 GPa, 27-185 MPa and 22-162 kJ/m^2 respectively, which are acceptable strength and modulus values similar to those of the human bone. Fixation plate with mechanical properties closer to

bone could prevent stress concentration on the bone and thus increase the required load to failure. Based on the results, it can be concluded that the GF/PP composites are good candidates for load-bearing during daily human physiological activities. The PPLGF shows an overall superiority as compared with the other types, due to the reinforcing effects of unidirectional rendered long fiber-glass and excellent mechanical properties. Thus, to improve the future application of the composite orthopedic fixation plate, PPLGF recommended as the first choice.

Nomenclature

M	Bending moment $(\boldsymbol{N.m})$	BS	Bending stiffness $(\boldsymbol{N.m/°})$
P	Applied load in four-point bending test $(\boldsymbol{N})$	θ	Bending angulation $(\boldsymbol{Degree}$ (°))
l	The length between the outer and inner rollers in four-point bending test$(\boldsymbol{m})$	δ	Deflection at the center of the fixation plate in four-point bending test $(\boldsymbol{m})$
$\bar{y}$	Position of the neutral axis $(\boldsymbol{m})$	ρ	Density $(\boldsymbol{Kg/m^3})$
I	the second moment of inertia of the cross-section $(\boldsymbol{m^4})$	τ	Shear stress $(\boldsymbol{MPa})$
E	Young's modulus$(\boldsymbol{GPa})$	ν	Poisson's ratio
G	Shear modulus$(\boldsymbol{GPa})$	σ_U^T	Ultimate tensile strength $(\boldsymbol{MPa})$
E_B	Bending modulus$(\boldsymbol{GPa})$	σ_U^C	Ultimate compressive strength $(\boldsymbol{MPa})$
IR	Impact resistance $(\boldsymbol{kJ/m^2})$	σ_U^B	Ultimate bending strength $(\boldsymbol{MPa})$

Appendix A:

FigureA.1 shows the axial strain patterns of the PPSCGF sample during tensile testing for example to prove the results of the DIC measurement method.

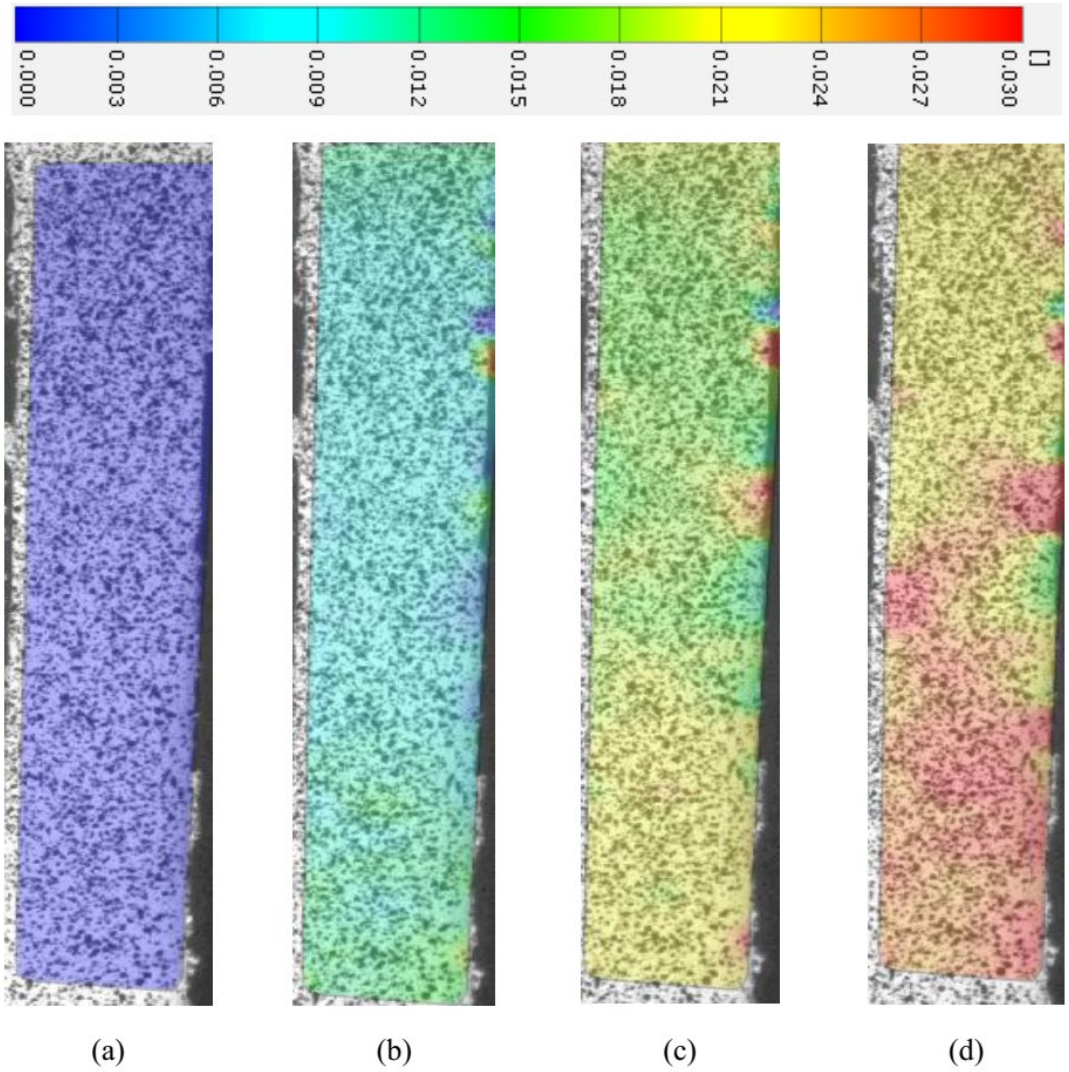

Figure A.1. DIC full field images of axial strain of the PPSCGF sample during tensile testing; a) time=1 (sec), b) time=10 (sec), c) time=20 (sec) and d) time=25 (sec).

Declaration of Conflicting Interests

The authors declared no potential conflicts of interest with respect to the research, authorship, and/or publication of this article.

Funding

The authors received no financial support for the research, authorship, and/or publication of this article.

5. References

1. Mantripragada VP, Lecka-Czernik B, Ebraheim NA, Jayasuriya AC. An overview of recent advances in designing orthopedic and craniofacial implants. *Journal of biomedical materials research Part A* 2013; 101: 3349-3364.

2. Mirzaei M, Alavi F, Allaveisi F, Naeini V, Amiri P. Linear and nonlinear analyses of femoral fractures: Computational/experimental study. *Journal of biomechanics* 2018; 79: 155-163.

3. Wolff J. Das gesetz der transformation der knochen. *DMW-Deutsche MedizinischeWochenschrift* 1893; 19: 1222-1224.

4. Alpert B, Seligson D. Removal of asymptomatic bone plates used for orthognathic surgery and facial fractures. *Journal of oral and maxillofacial surgery* 1996; 54: 618-621.

5. Ramakrishna S, Mayer J, Wintermantel E, Leong KW. Biomedical applications of polymer-composite materials: a review. *Composites science and technology* 2001; 61: 1189-1224.

6. Ali MS, French TA, Hastings GW, Rae T, Rushton N, Ross ER, Wynn-Jones CH. Carbon fibre composite bone plates. Development, evaluation and early clinical experience. *The Journal of bone and joint surgery. British volume* 1990; 72: 586-591.

7. Fujihara K, Huang ZM, Ramakrishna S, Satknanantham K, Hamada H. Feasibility of knitted carbon/PEEK composites for orthopedic bone plates. *Biomaterials* 2004; 25: 3877-3885.

8. Fujihara K, Huang ZM, Ramakrishna S, Satknanantham K, Hamada H. Performance study of braided carbon/PEEK composite compression bone plates. *Biomaterials* 2003; 24: 2661-2667.

9. Huang ZM, Fujihara K. Stiffness and strength design of composite bone plates. *Composites science and technology* 2005; 65: 73-85.

10. Schambron T, Lowe A, McGregor HV. Effects of environmental ageing on the static and cyclic bending properties of braided carbon fibre/PEEK bone plates. *Composites Part B: Engineering* 2008; 39: 1216-1220.

11. Steinberg EL, Rath E, Shlaifer A, Chechik O, Maman E, Salai M. Carbon fiber reinforced PEEK Optima—a composite material biomechanical properties and wear/debris characteristics of CF-PEEK composites for orthopedic trauma implants. *Journal of the mechanical behavior of biomedical materials* 2013; 17: 221-228.

12. Huda MS, Drzal LT, Mohanty AK, Misra M. Effect of fiber surface-treatments on the properties of laminated biocomposites from poly (lactic acid)(PLA) and kenaf fibers. *Composites science and technology* 2008; 68: 424-432.

13. Aydin E, Planell JA, Hasirci V. Hydroxyapatite nanorod-reinforced biodegradable poly (L-lactic acid) composites for bone plate applications. *Journal of Materials Science: Materials in Medicine* 2011; 22: 2413-2427.
14. Li X, Chu CL, Liu L, Liu XK, Bai J, Guo C, Xue F, Lin PH, Chu PK. Biodegradable poly-lactic acid based-composite reinforced unidirectionally with high-strength magnesium alloy wires. *Biomaterials* 2015; 49: 135-144.
15. Dos Santos TM, Merlini C, Aragones Á, Fredel MC. Manufacturing and characterization of plates for fracture fixation of bone with biocomposites of poly (lactic acid-co-glycolic acid)(PLGA) with calcium phosphates bioceramics. *Materials Science and Engineering: C* 2019; 103: 109728.
16. Taghizadeh SA, Liaghat G, Niknejad A, Pedram E. Experimental study on quasi-static penetration process of cylindrical indenters with different nose shapes into the hybrid composite panels. *Journal of Composite Materials* 2019; 53: 107-123.
17. Cadavid MO, Al-Khudairi O, Hadavinia H, Goodwin D, Liaghat GH. Experimental studies of stiffness degradation and dissipated energy in glass fibre reinforced polymer composite under fatigue loading. *Polymers and Polymer Composites* 2017; 25: 435-446.
18. Jiang G, Evans ME, Jones IA, Rudd CD, Scotchford CA, Walker GS. Preparation of poly (ε-caprolactone)/continuous bioglassfibre composite using monomer transfer moulding for bone implant. *Biomaterials* 2005; 26: 2281-2288.
19. Kobayashi HY, Brauer DS, Rüssel C. Mechanical properties of a degradable phosphate glass fibre reinforced polymer composite for internal fracture fixation. *Materials Science and Engineering: C* 2010; 30: 1003-1007.
20. Ahmed I, Jones IA, Parsons AJ, Bernard J, Farmer J, Scotchford CA, Walker GS, Rudd CD. Composites for bone repair: phosphate glass fibre reinforced PLA with varying fibre architecture. *Journal of Materials Science:Materials in Medicine* 2011; 22: 1825-1834.
21. Park SW, Yoo SH, An ST, Chang SH. Material characterization of glass/polypropylene composite bone plates according to the forming condition and performance evaluation under a simulated human body environment. *Composites Part B: Engineering* 2012; 43: 1101-1108.
22. Liesmäki O, Plyusnin A, Kulkova J, Lassila LV, Vallittu PK, Moritz N. Biostable glass fibre-reinforced dimethacrylate-based composites as potential candidates for fracture fixation plates in toy-breed dogs: Mechanical testing and finite element analysis. *Journal of the mechanical behavior of biomedical materials* 2019; 96: 172-185.

23. Hertel R, Eijer H, Meisser A, Hauke C, Perren SM. Biomechanical and biological considerations relating to the clinical use of the Point Contact-Fixator--evaluation of the device handling test in the treatment of diaphyseal fractures of the radius and/or ulna. *Injury* 2001; 32: B10-4.

24. Hedayati SK, Behravesh AH, Hasannia S, Saed AB, Akhoundi B. 3D printed PCL scaffold reinforced with continuous biodegradable fiber yarn: A study on mechanical and cell viability properties. *Polymer Testing* 2020: 106347.

25. Akhoundi B, Behravesh AH, BagheriSaed A. Improving mechanical properties of continuous fiber-reinforced thermoplastic composites produced by FDM 3D printer. *Journal of Reinforced Plastics and Composites* 2019; 38: 99-116.

26. ASTM D3039. Standard test method for tensile properties of polymer matrix composite materials. *Annual Book of ASTM Standards*2005.

27. ASTM D638. Standard Test Method for Tensile Properties of Plastics. *Annual Book of ASTM Standards*2002.

28. ASTM D3518. Standard Test Method for In-Plane Shear Response of Polymer Matrix Composite Materials by Tensile Test of a ±45° Laminate. *Annual Book of ASTM Standards* 2001.

29. ASTM D3410. Standard Test Method for Compressive Properties of Polymer Matrix Composite Materials with Unsupported Gage Section by Shear Loading. *Annual Book of ASTM Standards* 2003.

30. ASTM D7264. Standard Test Method for Flexural Properties of Polymer Matrix Composite Materials. *Annual Book of ASTM Standards* 2007.

31. ASTM D6110. Standard Test Method for Determining the Charpy Impact Resistance of Notched Specimens of Plastics. *Annual Book of ASTM Standards* 2004.

32. Brydone AS, Meek D, Maclaine S. Bone grafting, orthopaedic biomaterials, and the clinical need for bone engineering. *Proceedings of the Institution of Mechanical Engineers, Part H: Journal of Engineering in Medicine* 2010; 224: 1329-1343.

33. Simkin A, Robin G. The mechanical testing of bone in bending. *Journal of biomechanics* 1973; 6: 31-39.

34. Kim SH, Chang SH, Jung HJ. The finite element analysis of a fractured tibia applied by composite bone plates considering contact conditions and time-varying properties of curing tissues. *Composite Structures* 2010; 92: 2109-2118.

35. Guo Y, Zhu S, Chen Y, Li D. Analysis and Identification of the Mechanism of Damage and Fracture of High-Filled Wood Fiber/Recycled High-Density Polyethylene Composites. *Polymers* 2019; 11: 170.
36. Glória GO, Margem FM, Ribeiro CG, Moraes YM, Cruz RB, Silva FD, Monteiro SN. Charpy impact tests of epoxy composites reinforced with giant bamboo fibers. *Materials Research* 2015; 18: 178-184.
37. ASTM D792. Standard Test Methods for Density and Specific Gravity (Relative Density) of Plastics by Displacement. *Annual Book of ASTM Standards* 2004.
38. Charlet K, Jernot JP, Gomina M, Bizet L, Bréard J. Mechanical properties of flax fibers and of the derived unidirectional composites. *Journal of Composite Materials* 2010; 44: 2887-2896.
39. Gning PB, Liang S, Guillaumat L, Pui WJ. Influence of process and test parameters on the mechanical properties of flax/epoxy composites using response surface methodology. *Journal of materials science* 2011; 46: 6801-6811.
40. Lamy B, Baley C. Stiffness prediction of flax fibers-epoxy composite materials. *Journal of materials science letters* 2000; 19: 979-980.
41. Manteghi S, Mahboob Z, Fawaz Z, Bougherara H. Investigation of the mechanical properties and failure modes of hybrid natural fiber composites for potential bone fracture fixation plates. *Journal of the mechanical behavior of biomedical materials* 2017; 65: 306-316.
42. Bagheri ZS, El Sawi I, Schemitsch EH, Zdero R, Bougherara H. Biomechanical properties of an advanced new carbon/flax/epoxy composite material for bone plate applications. *Journal of the mechanical behavior of biomedical materials* 2013; 20: 398-406.
43. Kotela I, Chlopek J, Rosol P, Blazewicz M. Mechanical assessment of non-metallic composite clamps designed for orthopaedic surgery. *Journal of composite materials* 2009; 43: 3265-3274.
44. Fiore VI, Di Bella G, Valenza A. Glass–basalt/epoxy hybrid composites for marine applications. *Materials & Design* 2011; 32: 2091-2099.
45. Khanam PN, Khalil HA, Jawaid M, Reddy GR, Narayana CS, Naidu SV. Sisal/carbon fibre reinforced hybrid composites: tensile, flexural and chemical resistance properties. *Journal of Polymers and the Environment* 2010; 18: 727-733.
46. Moritz N, Strandberg N, Zhao DS, Mattila R, Paracchini L, Vallittu PK, Aro HT. Mechanical properties and in vivo performance of load-bearing fiber-reinforced composite

intramedullary nails with improved torsional strength. *Journal of the mechanical behavior of biomedical materials* 2014; 40: 127-139.

47. Wojcieszak M, Percot A, Colomban P. Regenerated silk matrix composite materials reinforced by silk fibres: relationship between processing and mechanical properties. *Journal of Composite Materials 2018*; 52: 2301-2311.

48. Bougherara H, Saleem M, Shah S, Toubal L, Sarwar A, Schemitsch EH, Zdero R. Stress analysis of a carbon fiber-reinforced epoxy plate with a hole undergoing tension: A comparison of finite element analysis, strain gages, and infrared thermography. *Journal of Composite Materials* 2018; 52: 2679-2689.

49. Kim JH, Kim SH, Chang SH. Estimation of the movement of the inter-fragmentary gap of a fractured human femur in the presence of a composite bone plate. *Journal of composite materials* 2011; 45: 1491-1498.

50. Moreno KJ, García-Miranda JS, Hernandez-Navarro C, Ruiz-Guillen F, Aguilera-Camacho LD, Lesso R, Arizmendi-Morquecho A. Preparation and performance evaluation of PMMA/HA nanocomposite as bulk material. *Journal of Composite Materials* 2015; 49: 1345-1353.

51. Kharazi AZ, Fathi MH, Bahmani F, Fanian H. Nonmetallic textile composite bone plate with desired mechanical properties. *Journal of composite materials* 2012; 46: 2753-2761.

52. Popescu LM, Rusti CF, Piticescu RM, Buruiana T, Valero T, Kintzios S. Synthesis and characterization of acid polyurethane–hydroxyapatite composites for biomedical applications. *Journal of composite materials* 2013; 47: 603-612.

53. Rakmae S, Ruksakulpiwat Y, Sutapun W, Suppakarn N. Physical properties and cytotoxicity of surface-modified bovine bone-based hydroxyapatite/poly (lactic acid) composites. *Journal of composite materials* 2011; 45: 1259-1269.

54. Shubhra QT, Alam AK, Beg MD, Khan MA, Gafur MA. Mechanical and degradation characteristics of natural silk and synthetic phosphate glass fiber reinforced polypropylene composites. *Journal of composite materials* 2011; 45: 1305-1313.

55. Younesi M, Bahrololoom ME. Effect of molecular weight, particle size and ringer's solution on mechanical properties of surface-treated polypropylene-hydroxyapatite biocomposites. *Journal of composite materials* 2010; 44: 2785-2799.

56. Younesi M, Bahrololoom ME. Effect of polypropylene molecular weight, hydroxyapatite particle size, and Ringer's solution on creep and impact behavior of polypropylene-surface treated hydroxyapatite biocomposites. *Journal of composite materials*. 2011; 45: 513-523.

57. Ansari M, Golzar M, Baghani M, Soleimani M. Shape memory characterization of poly (ε-caprolactone) (PCL)/polyurethane (PU) in combined torsion-tension loading with potential applications in cardiovascular stent. *Polymer Testing* 2018; 68: 424-432.
58. Abbasi-Shirsavar M, Baghani M, Taghavimehr M, Golzar M, Nikzad M, Ansari M, George D. An experimental–numerical study on shape memory behavior of PU/PCL/ZnO ternary blend. *Journal of Intelligent Material Systems and Structures* 2019; 30: 116-126.
59. Ansari M, Golzar M, Baghani M, Abbasishirsavar M, Taghavimehr M. Force recovery evaluation of thermo-induced shape-memory polymer stent: Material, process and thermo-viscoelastic characterization. *Smart Materials and structures* 2019; 28: 095022.